

Isotactic polypropylene, β -phase: a study in frustration

D. L. Dorset^{a,*}, M. P. McCourt^a, S. Kopp^b, M. Schumacher^b, T. Okihara^b and B. Lotz^b

^aElectron Diffraction Department, Hauptman-Woodward Medical Research Institute, 73 High Street, Buffalo, NY 14203-1196, USA

^bInstitut Charles Sadron (CNRS-ULP), 6 rue Boussingault, F-67083 Strasbourg, France
 (Received 25 August 1997; revised 26 September 1997)

The three-dimensional crystal structure of isotactic polypropylene in its β -polymorphic form has been refined against electron diffraction intensity data. Microtwinning by merohedry, probably in two antichiral domains in space groups $P3_1$ and $P3_2$, was identified by sharp continuous diffraction in $h0l$ patterns from epitaxially crystallized samples. Nevertheless, a rather simple model of a frustrated chain packing could be improved by Fourier methods even though the solution of the structure by direct methods was itself frustrated by the extensive overlap of $|F_{hk0}|$ and $|F_{k0h}|$ or $|F_{hke}|$ and $|F_{hk,-e}|$ amplitudes which led initially to a false prediction of space group symmetry. © 1998 Elsevier Science Ltd. All rights reserved.

(Keywords: isotactic polypropylene; β -polymorphic form; frustrated chain packing)

INTRODUCTION

As reviewed recently¹, isotactic polypropylene is a synthetic polymer that exhibits unusual crystallization properties, many of which have only recently been understood in terms of underlying crystal structures. Although the lamellar chain packing of the α -polymorph has been known for over 30 years², the mechanism for 'quadrite'-type dendritic growth³ was only described in 1986 by Lotz and Wittmann⁴. This unusual dendrite formation is nucleated on a crystal face in a way that also explains⁵ the formation of the γ -polymorph, a unique crystal structure where pairs of antichiral polymer chains are actually layered cross-wise in the unit cell⁶.

Although the β -polymorph of this polymer was originally identified nearly 40 years ago⁷, its crystal structure has also remained a puzzle until recently. Turner-Jones and Cobbold⁸ proposed it to involve a hexagonal chain packing, an arrangement difficult to rationalize for domains of strictly chiral helices. Almost simultaneously, two similar models were proposed for the polymer as a frustrated array similar to a dual Kagomé lattice^{9,10}. Nevertheless, there remains some uncertainty about the actual space group of this crystal form, not to mention the need for a more accurate determination of the chain packing geometry.

The refined crystal structure of β -isotactic polypropylene is described in this paper, based on the measurement of 88 unique three-dimensional electron diffraction intensities.

MATERIALS AND METHODS

Crystallization

The polymer was crystallized in two orthogonal orientations in the presence of a small molecule, γ -chinacridone, that nucleates the β -polymorph. Both crystallizations start

with the nucleation of a thin polymer film from its melt at 135°C. For the form expressing the 'face-on' lamellar surfaces, tiny crystals of the nucleating agent were sprayed on to the polymer film before the thin layer was melted and recrystallized. Larger nucleator crystals (tens of micrometres in lateral dimension) were placed over the polymer film to express the orthogonally crystallized orientation by epitaxial nucleation, according to the principles established by Wittmann and Lotz¹¹.

Electron diffraction and intensity measurement

Selected area electron diffraction patterns were obtained at 100 kV with a JEOL JEM-100CXII and at 120 kV with a Philips CM-12, both electron microscopes equipped with side-entry goniometer stages. With a rotation holder, it was possible to orient specific reciprocal axes of the polymer crystal for observation of specific tilted planes of the reciprocal lattice (see Dorset¹²). Electron diffraction patterns were recorded on X-ray films, e.g. Kodak DEF-5, and the diffraction camera lengths were calibrated with gold powder diffraction standards.

Diffraction patterns from face-on views of the polymer chain-folded lamellae were then evaluated with the computer program ELDIF¹³ after they were digitized with a fast CCD camera via a frame-grabber into an IBM 433 DX personal computer. To establish that the intensities from equivalent measurements from different microcrystals were self-consistent, we evaluated the figure of merit¹⁴:

$$R_{\text{merge}} = \frac{\sum (|F_{hk0}|^{\text{pattern } 1} - k|F_{hk0}|^{\text{pattern } 2}) / \sum |F_{hk0}|^{\text{pattern } 1}}$$

Because of the limited dynamic range of the fast CCD camera, a more accurate measurement of intensities was made by integrating scans with a Joyce-Loebl Mk. III C flat-bed microdensitometer—a procedure carried out for

* To whom correspondence should be addressed

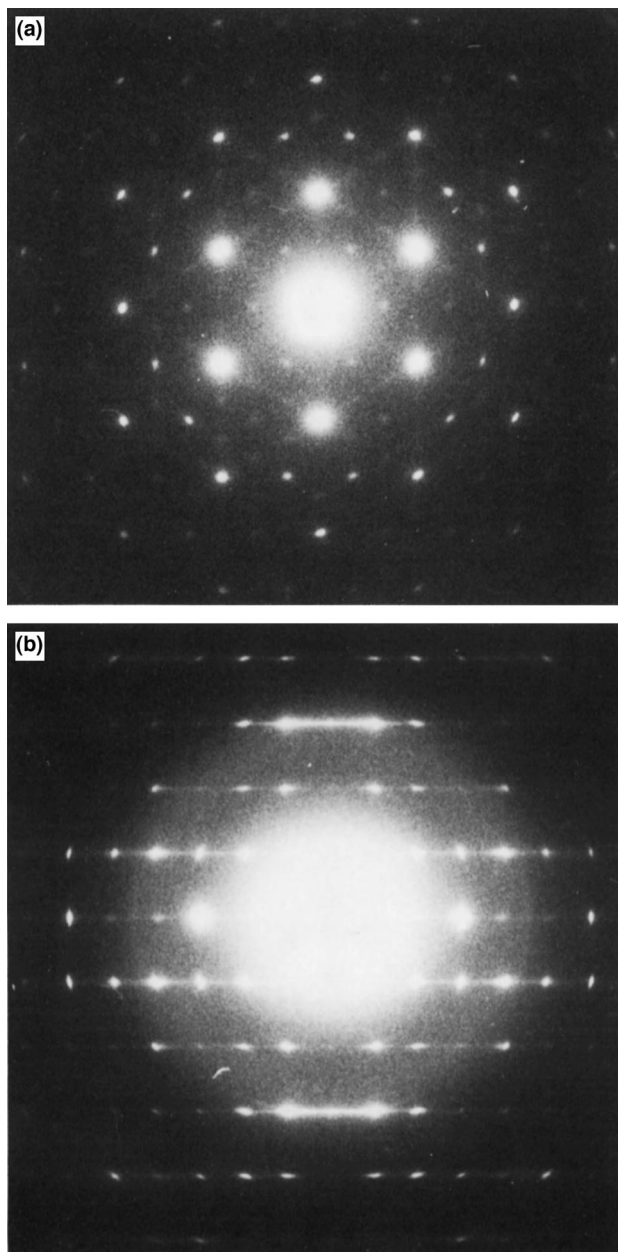


Figure 1 Electron diffraction patterns from β -phase isotactic polypropylene. (a) $hk0$ from face-on lamellae—note ‘Star of David’ diffuse scattering motif. (b) $h0\ell$ pattern from epitaxially oriented samples—note sharp, intense continuous streaks parallel to a^*

all tilted projections, in addition to the $hk0$ and $h0\ell$ patterns observed, respectively, from face-on and edge-on lamellae. For reasons discussed earlier¹², no Lorentz correction was made to the observed intensity values. For comparison of equivalent patterns, R_{merge} was generally less than 0.11.

Attempted phase determination

Direct methods were used in an attempt to phase the $hk0$ structure factor amplitudes from this polymer form. Three phase Σ_2 invariants¹⁵ were generated, followed by a convergence procedure¹⁶ to determine how the greatest number of phases could be accessed by the least number of defining reflections in the basis set—an important consideration since many or all $hk0$ reflections are invariants for the trigonal and hexagonal space groups¹⁷. Algebraic phase values were assigned to the (110), (300) and (350) reflections to generate 16 possible solutions in one enantiomorphic set via the Sayre equation¹⁸. The plane

group was assumed to be $p31m$ (see below). Possible solutions were identified with the ‘peakiness’ criterion¹⁹, i.e. seeking a maximum value for $\sum_i \rho_i^5$, where ρ_i is pixel density within the map.

Fourier refinement

After the correct space group was identified (see below), a model suggested for the frustrated chain packing¹⁰ was refined by Fourier techniques in three dimensions. For calculation of crystallographic residuals, it was assumed that overlapped reflections containing incoherent contributions from microtwins in two antichiral orientations could be partitioned equally so that:

$$((I_1^{\text{calc}} + I_2^{\text{calc}})/2)^{1/2} = \langle |F_{1,2}^{\text{calc}}| \rangle$$

Atomic positions within the three unit chain positions identified in the potential maps were then used for successive structure factor calculations and their phases assigned to the averaged amplitudes for calculation of successive potential maps.

RESULTS

Evaluation of electron diffraction patterns

Electron diffraction patterns were measured to verify the previously observed unit cell constants⁹: $a = b = 11.03$, $c = 6.50$ Å, $\gamma = 120^\circ$. The c -spacing was remeasured both from tilt diffraction series around a^* and from $h0\ell$ patterns from epitaxially oriented samples.

Two apparent amplitude relationships are observed to high precision for experimental data. First, in the face-on view of lamellae (Figure 1a): $|F_{hk0}| = |F_{kh0}|$. From both tilted face-on lamellar samples (equal inclination angles from the $hk0$ net) and epitaxial samples, e.g. the $h0\ell$ pattern in Figure 1b: $|F_{hk\ell}| = |F_{hk,-\ell}|$. In addition, from observed $h0\ell$ patterns, systematic absences appear for all reflections in the 00ℓ row except for $\ell = 3n$.

To assemble a unique three-dimensional intensity set with 88 reflections, reflections from tilted face-on lamellae and epitaxial layers (here $h0\ell$ and $hh\ell$) were combined, scaling according to common reflections²⁰. There was excellent agreement between equivalent $hk\ell$ intensities collected from tilted lamellae or epitaxially oriented samples, supporting the existence of a common crystal structure.

A Wilson plot made from the combined data set predicted the overall temperature factor to be $B_{\text{iso}} = 2.2$ Å². After calculation of normalized structure factors $|E_h|$, their distribution was compared to theoretical values²¹, shown in Table 1, to support a noncentrosymmetric crystal structure.

An attempted crystal structure analysis

Before three-dimensional intensities were collected from tilted lamellae and/or epitaxial preparations, an attempt was made to solve the packing of the [001] projection by direct methods. The amplitude relationship $|F_{hk0}| = |F_{kh0}|$ points to the plane group $p31m$ as a likely symmetry for this projection, agreeing also with an earlier proposal⁹. After generation of multiple phase sets via the Sayre equation, the potential map in Figure 2 was found to be a likely solution. Although average atomic positions were clearly indicated in this map, the solution is geometrically impossible, especially for polymer chains at the unit cell apices, and also violates the expectations for a close packed structure²².

Table 1 $|E_h|$ distributions for isotactic polypropylene

	Expt.	Centrosym.	Non-centrosym.
$\langle E_h ^2 \rangle$	1.000	1.000	1.000
$\langle E_h^2 - 1 \rangle$	0.643	0.968	0.736
$\langle E_h \rangle$	0.919	0.798	0.886
$ E_h > 1, \%$	33.0	32.0	36.8
$ E_h > 2, \%$	1.1	5.0	1.8
$ E_h > 3, \%$	0.0	0.3	0.01

Nevertheless, the crystallographic residual ($R = 0.26$), measuring the fit of the model to 38 unique $hk0$ amplitudes, appeared to be 'reasonable'.

Attempts made to improve the structural model by rotational searches with the apical chains were unsuccessful since they resulted in higher R -values as well as unresolved atomic positions in the potential maps calculated from the new crystallographic phase values. Similar attempts were made to solve the structure in plane group $p6mm$, where the amplitude relationship also holds, but these trials always resulted in significantly higher values of the crystallographic residual than found with the solution in plane group $p31m$.

Identification of the space group

After collection of three-dimensional data and noting that $|F_{hk\ell}| = |F_{hk,-\ell}|$, also observed in the earlier work⁹, it was found that no trigonal space group would fit all the conditions listed above, including $\ell = 3n$ for the 00ℓ row. (The latter extinction rule was not noted in the earlier study because of the non-availability of epitaxially oriented specimens.) In the previous three-dimensional study⁹, an orthorhombic space group $C2cm$ (i.e. $a = 11.03$, $b = 19.08$, $c = 6.49$ Å) was proposed to account for the amplitude identities. However, inspection of our $h0\ell$ patterns (Figure 1b), again, clearly revealed that $\ell = 3n$, contradicting the $\ell = 2n$ rule required for 00ℓ reflections in the orthorhombic symmetry group. The only space groups that matched all constraints on the data were hexagonal: $P6_222$ or $P6_422$. However, we have already shown that the projected $p6mm$ plane group does not lead to a model that adequately matches the observed $|F_{hk0}|$ diffracted amplitudes.

This dilemma was resolved by inspection of Figure 1b. Strong sharp, continuous diffraction streaks were found parallel to the a^* in $h0\ell$ patterns. Because of the $\text{sinc}(\pi t u)$ relationship for a width t , this indicated the presence of thin 'cigarello' domains²³ with polarities aligned parallel or antiparallel to the lamellar surface normal. If each thin domain were to pack in space group $P3_1$ or $P3_2$, this would account for the observed relationship $|F_{hk\ell}| = |F_{hk,-\ell}|$, due to overlap of nonequivalent reflections at identical values of d^* . The existence of twinning by merohedry for trigonal space groups is well known²⁴. Such twinning, moreover, would place diffraction spots exactly over one another. If this co-packing of domains in a coherently microtwinning structure would also cause an accidental mirroring of an average lattice around $\langle 110 \rangle$, then $|F_{hk0}| = |F_{kh0}|$ would also be observed. Nevertheless, the twin laws for merohedry²⁵ supported our observation that intensity distributions consistent with space group $P6_222$ were really caused by a lower symmetry group such as $P3_1$.

Fourier refinement of a frustrated chain packing

A previously proposed frustrated chain packing¹⁰, shown in Figure 3, was used as a starting point for a Fourier refinement. A structurally conservative chain helix²⁶ in point group 3_1 was constructed and placed into three unique

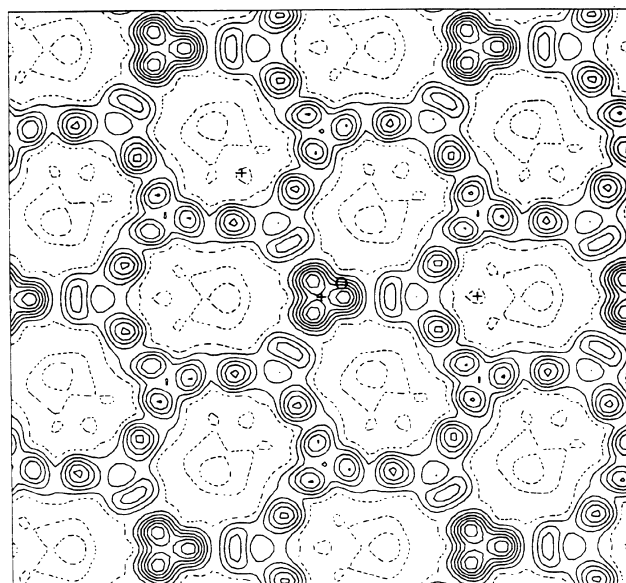


Figure 2 Model from direct phasing of isotactic polypropylene $hk0$ data assuming $p31m$ plane group symmetry

positions of the unit cell ($0,0; 2/3,1/3; 1/3,2/3$; for the $[001]$ projection) according to the methyl group elevations suggested in our earlier work¹⁰. Structure factor calculations in $P3_1$ provided unique phase information to observed $|F_{hk0}|$ and $|F_{kh0}|$ pairs, as well as $|F_{hk\ell}|$ and $|F_{hk,-\ell}|$ pairs, while their amplitudes were held at the average values defined above. In other words, the microtwinning phenomenon was assumed to be an incoherent disorder. Potential maps calculated from these combinations of phases and amplitudes were used to find atomic coordinates for a new structure factor calculation, etc. (In this work, other starting models⁹ were also evaluated.)

The final model for the polymer chain packing in space group $P3_1$ is shown in Figures 4 and 5. The azimuthal changes of chains from the starting position (Figure 3) are to be noted. After optimizing the fit of bond distances and angles within the density envelope (coordinate list given in Table 2 and bonding parameters in Figure 6), the fit of the model ($B_{\text{iso}} = 4.0$ Å² for all atoms) to the 88 unique reflections (Table 3) was $R = 0.33$, if $|F_{\text{calc}}|$ values were not overlapped, and $R = 0.22$, if they were. The significance of this final residual could be tested using procedures outlined by Hamilton²⁷. Given a significance level of 0.05, the new structure could be justified when seven variables (three torsional and three longitudinal parameters for the chains and one overall temperature factor) were refined against 88 measured intensities. The model could not be distinguished from the starting point if nine independent atomic positions (three positional shifts each and an overall temperature factor) were refined against these data, even though $R = 0.28$ for the packing in Figure 3, after overlapping antichiral contributions to diffracted intensity were taken into account.

Diffuse scattering in the $hk0$ pattern

The characteristic 'Star of David' motif for continuous diffuse scattering in the $hk0$ pattern (Figure 1a), originally observed by Turner-Jones and Cobbold⁸ was found to be a consequence of the disordered chain packing. It is weaker and more diffuse than the streaking of $h0\ell$ pattern that was used to identify the type of crystalline disorder. Explanation

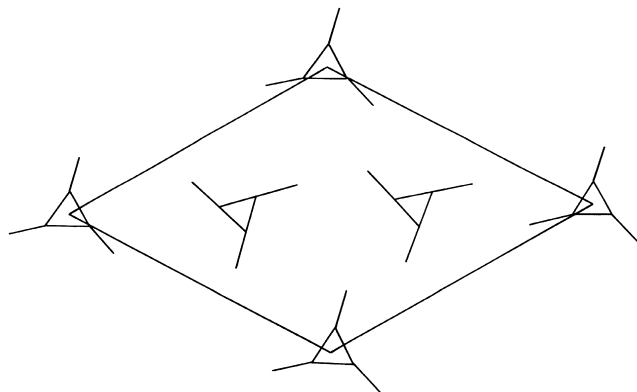


Figure 3 Frustrated chain packing model in space group $P3_1$ proposed by Lotz *et al.*¹⁰

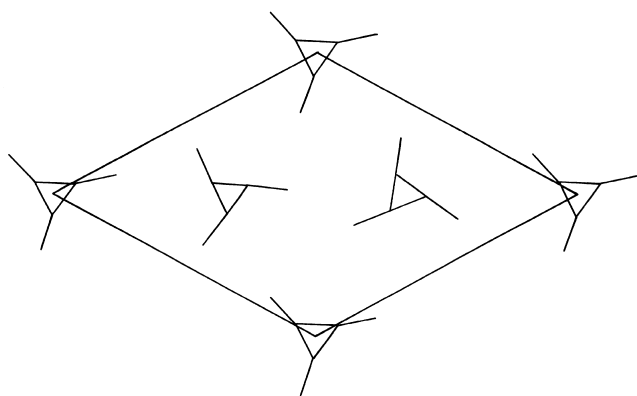


Figure 4 Refined model of isotactic polypropylene, [001] projection

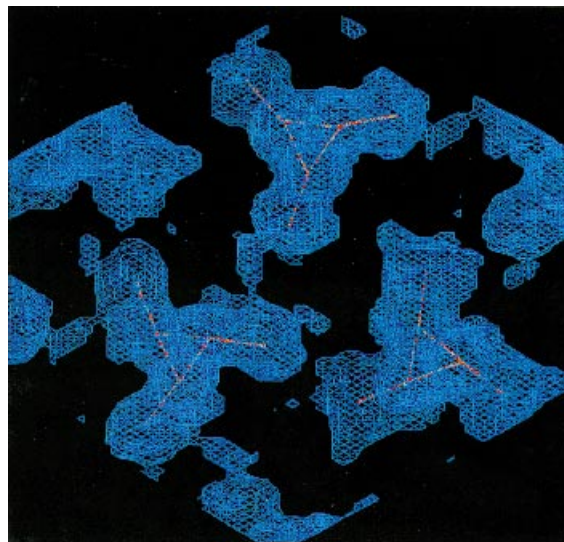
Table 2 Carbon fractional coordinates for isotactic polypropylene

Atom	x/a	y/b	z/c
1	0.2311	0.1785	0.5951
2	0.0823	0.0772	0.6740
3	0.0696	0.0692	0.9104
4	0.5426	0.6813	0.4169
5	0.4199	0.6977	0.4958
6	0.4169	0.6991	0.7328
7	0.8910	0.4606	0.6334
8	0.7410	0.4004	0.7168
9	0.7444	0.4040	0.9538

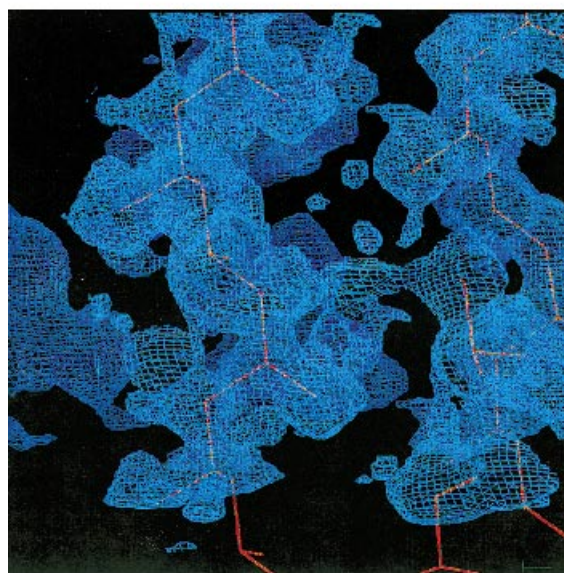
of such continuous diffraction intensity with a disorder model can be somewhat non-specific²⁸. At least two models could satisfy the placement of intensity between the major Bragg peaks. If, for example, a thermal (or static displacement) model²³ was used to calculate such intensity in plane group symmetry $p31m$ via:

$$I_{TDS} = I_{hk0} \left\{ 1 - \exp \left(- \frac{1}{2} B |r^*|^2 \right) \right\}$$

then a reasonable match to experiment could be demonstrated (Figure 7). It was assumed that scattering for all contents of the unit cell was correlated. Alternatively, a random mixture of polar structures, corresponding to the microtwinning phenomenon proposed above could also produce a similar diffuse scattering signal. Work is currently in progress to resolve the true disorder mechanism.



(a)



(b)

Figure 5 Refined model of isotactic polypropylene, three-dimensional map: (a) view on to chains; (b) view down chain axes

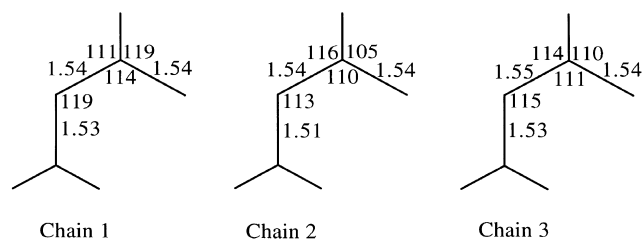


Figure 6 Bond distances and angles for three unique chain repeats

DISCUSSION

It has become increasingly apparent²⁹ that frustrated lattices are characteristic of many chiral polymer crystal structures. As shown in the projected structure of β -isotactic polypropylene in Figure 4, the chains cannot adopt a simple close packing scheme in the trigonal unit cell to minimize the non-bonded energy, whereas the combination of enantiomers in the same unit cell will lead to a more

Table 3 Final observed and calculated structure factors, β -i-polypropylene

hkl	Fobs	Fcalc	hkl	Fobs	Fcalc
100	0.35	0.08	$\langle 302 \rangle$	0.23	0.14
200	0.33	0.15	$\langle 402 \rangle$	0.36	0.40
300	1.35	1.25	$\langle 502 \rangle$	0.16	0.18
400	0.35	0.40	$\langle 602 \rangle$	0.14	0.14
500	0.24	0.27	$\langle 702 \rangle$	0.12	0.10
600	0.49	0.43	$\langle 112 \rangle$	0.43	0.49
700	0.15	0.19	$\langle 312 \rangle$	0.34	0.36
110	2.53	2.96	$\langle 222 \rangle$	0.44	0.45
$\langle 210 \rangle$	0.74	0.76	$\langle 332 \rangle$	0.28	0.19
$\langle 310 \rangle$	0.35	0.43	$\langle 442 \rangle$	0.19	0.09
$\langle 410 \rangle$	0.54	0.38	003	0.65	0.78
$\langle 510 \rangle$	0.24	0.36	$\langle 103 \rangle$	1.06	0.94
$\langle 610 \rangle$	0.22	0.23	$\langle 203 \rangle$	0.59	0.50
$\langle 710 \rangle$	0.31	0.41	$\langle 303 \rangle$	0.19	0.28
220	1.06	0.60	$\langle 403 \rangle$	0.23	0.15
$\langle 320 \rangle$	0.35	0.40	$\langle 503 \rangle$	0.16	0.19
$\langle 420 \rangle$	0.29	0.32	$\langle 603 \rangle$	0.12	0.17
$\langle 520 \rangle$	0.40	0.47	$\langle 703 \rangle$	0.17	0.16
$\langle 620 \rangle$	0.21	0.25	$\langle 113 \rangle$	0.38	0.40
330	0.51	0.50	$\langle 223 \rangle$	0.22	0.37
$\langle 430 \rangle$	0.28	0.24	$\langle 333 \rangle$	0.19	0.23
$\langle 530 \rangle$	0.26	0.36	$\langle 104 \rangle$	0.37	0.24
$\langle 630 \rangle$	0.37	0.30	$\langle 204 \rangle$	0.42	0.33
440	0.41	0.61	$\langle 304 \rangle$	0.30	0.32
$\langle 540 \rangle$	0.24	0.28	$\langle 404 \rangle$	0.25	0.13
$\langle 101 \rangle$	0.28	0.34	$\langle 504 \rangle$	0.37	0.27
$\langle 201 \rangle$	0.87	0.82	$\langle 604 \rangle$	0.15	0.20
$\langle 301 \rangle$	0.67	1.11	$\langle 704 \rangle$	0.12	0.11
$\langle 401 \rangle$	0.81	0.47	$\langle 114 \rangle$	0.23	0.32
$\langle 501 \rangle$	0.45	0.50	$\langle 224 \rangle$	0.23	0.35
$\langle 601 \rangle$	0.42	0.27	$\langle 334 \rangle$	0.21	0.29
$\langle 701 \rangle$	0.16	0.17	$\langle 105 \rangle$	0.12	0.04
$\langle 111 \rangle$	1.76	1.67	$\langle 205 \rangle$	0.15	0.12
$\langle 211 \rangle$	0.69	0.42	$\langle 305 \rangle$	0.27	0.28
$\langle 311 \rangle$	0.53	0.53	$\langle 405 \rangle$	0.20	0.18
$\langle 411 \rangle$	0.77	0.79	$\langle 505 \rangle$	0.13	0.11
$\langle 511 \rangle$	0.25	0.39	$\langle 605 \rangle$	0.12	0.09
$\langle 221 \rangle$	0.80	0.72	$\langle 115 \rangle$	0.18	0.09
$\langle 321 \rangle$	0.66	0.54	$\langle 225 \rangle$	0.22	0.28
$\langle 521 \rangle$	0.32	0.24	$\langle 335 \rangle$	0.16	0.15
$\langle 331 \rangle$	0.56	0.49	006	0.16	0.12
$\langle 441 \rangle$	0.25	0.18	$\langle 106 \rangle$	0.13	0.05
$\langle 102 \rangle$	0.63	0.56	$\langle 206 \rangle$	0.12	0.03
$\langle 202 \rangle$	0.41	0.32	$\langle 306 \rangle$	0.18	0.07

favourable packing scheme (e.g. the α -polymorphic form cited above). (An AFM study of epitaxial films, also supporting the concept of a frustrated structure via a 19 Å periodicity, is nearly completed (Lotz *et al.*, unpublished data).) The model of this polymer chain packing found by Fourier refinement, in fact, closely resembles the crystal structure of poly(2-vinylpyridine) reported by Puterman *et al.*³⁰, particularly in the arrangement of projected trimer positions for three independent molecules in a $P3_1$ unit cell. Relative rotational aspects of the independent polymer chains are also somewhat similar to the original model proposed by Meille *et al.*⁹ in their *Figure 6a*.

It is the disorder of this structure that leads to another,

methodological, frustration and that is the determination of the crystal structure from recorded electron diffraction patterns, despite the appearance of well-resolved single crystal intensities. False indications of equivalent amplitudes lead to an incorrect assignment of the space group symmetry and hence frustrates all attempts to solve the structure *ab initio* by direct methods. The presence of sharp streaks in $h0\ell$ electron diffraction patterns from epitaxially oriented samples (*Figure 1b*), unavailable unfortunately to the earliest three-dimensional study⁹, was the major clue that a microtwinning of a polar structure by merohedry was an important feature of the average structure and that a less symmetric trigonal cell, incorporating the point group

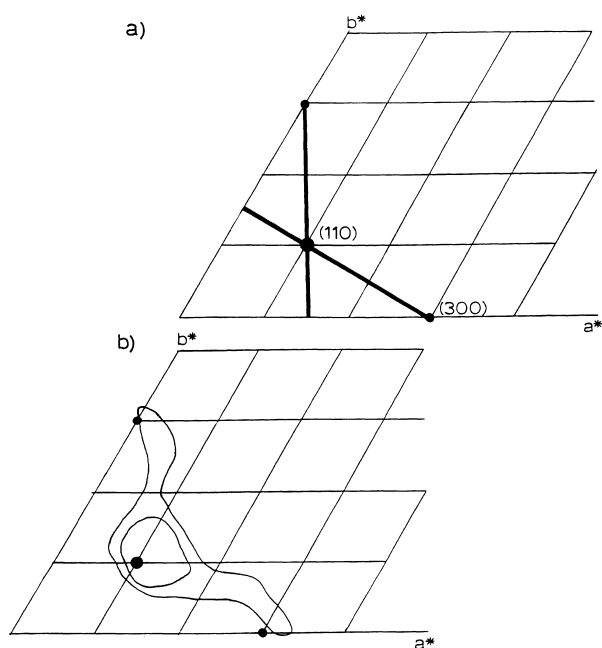


Figure 7 Match of (a) observed TDS model for diffuse scattering to (b) experimental location in average plane group $p31m$ —see *Figure 1a*

symmetry of the chain, must be the true form of the chiral domains. The microtwinning of two antichiral packing motifs, therefore, causes the lamellar packing to be finely divided into thin microdomains. Although some continuous scattering is observed in the $h\ell\ell$ patterns, the strongest streaks are observed for $h0\ell$. If the average combined packing were also mirrored across $\langle 110 \rangle$, for example, a repeat of antipolar domains along $\langle 210 \rangle$ would explain the strong streaks parallel to a^* and account for the apparent averaged $p31m$ plane group symmetry of the $[001]$ projection. Correlated overlap of non-equivalent hkl and $hk, -\ell$ reflections from the $P3_1$ and $P3_2$ domains would also account for these observed equivalences.

This postulate, however, does not entirely explain the nature of the twin. Twinning by merohedry in trigonal lattices is also well known in protein crystallography^{31,32}, but it is obvious in that case that the twinning operation must involve a 180° rotation (e.g. around a^* or $\langle 1, -1, 0 \rangle$), since antichirality is not possible in native biomolecules. On the other hand, other materials, such as α -quartz, in its Brazil twin³³, co-packs two oppositely handed structures in space groups $P3_121$ and $P3_221$. Aside from the twin direction in isotactic polypropylene being orthogonal to those proposed for the proteins or quartz (to preserve the average $p31m$ plane group symmetry in the $[001]$ projection), it is also clear, by inference from the other polymorphic forms, that domains of opposite handedness must exist in any crystal structure. Given accurate enough intensity data, it may be possible also to determine the average contribution of both chiral forms³¹, an enterprise that will be left for future consideration.

Finally, it is well known³⁴ that correct crystallographic phases are more important than accurate amplitudes for structure determination. Although direct structure determination was foiled by false intensity equivalences, equipartitioning of intensities between the overlapped reflections did not hinder the progress of a Fourier refinement, given the existence of an adequate starting model for atomic positions. The whole exercise serves as a cautionary note to anyone carrying out a crystal structure determination—

i.e. to observe the characteristics of all recorded diffraction data, including the continuous signal linking Bragg peaks, a point also made nearly 40 years ago²⁴.

ACKNOWLEDGEMENTS

Research was supported in part by a grant (to DLD) from the National Science Foundation (CHE94-17835) which is gratefully acknowledged. M. Schumacher was supported by a grant from Exxon Chemical International and T. Okihara acknowledges support from the CNRS and the Japanese Ministry of Education. One of us (DLD) also acknowledges fruitful discussions of this problem with Dr S. V. Meille, including his presentation of energy calculations for various choices of space group (NATO ASI on Electron Crystallography held at Erice, Sicily, 22 May to 2 June 1997), favouring $P3_1$ as one of the most probable space groups. Also, thanks are due to Dr G. D. Smith for discussing his recent work on the twinning of a trigonal form of insulin as well as for pointing out related literature in the protein field.

REFERENCES

1. Lotz, B., Wittmann, J. C. and Lovinger, A. J., *Polymer*, 1996, **37**, 4979–4992.
2. Natta, G. and Corridini, P., *Nuovo Cimento*, 1960, **15**(Suppl 1), 40–51.
3. Khoury, F., *J. Res. Natl. Bur. Standards*, 1966, **70A**, 29–61.
4. Lotz, B. and Wittmann, J. C., *J. Polym. Sci. B. Polym. Phys.*, 1986, **24**, 1541–1558.
5. Stocker, W., Magonov, S. N., Cantow, H. J., Wittmann, J. C. and Lotz, B., *Macromolecules*, 1993, **23**, 5915–5923.
6. Brückner, S. and Meille, S. V., *Nature (London)*, 1989, **340**, 455–457.
7. Keith, H. D., Padden, F. J. Jr., Walter, N. M. and Wickoff, H. W., *J. Appl. Phys.*, 1959, **30**, 1485–1488.
8. Turner-Jones, A. and Cobbold, A., *J. Polym. Sci.*, 1968, **B6**, 539–546.
9. Meille, S. V., Ferro, D. R., Brückner, S., Lovinger, A. J. and Padden, F. J. Jr., *Macromolecules*, 1994, **27**, 2615–2622.
10. Lotz, B., Kopp, S. and Dorset, D. L., *Compt. Rend. Acad. Sci. (Paris) Ser. IIb*, 1994, **319**, 187–192.
11. Wittmann, J. C. and Lotz, B., *Prog. Polym. Sci.*, 1990, **15**, 909–948.
12. Dorset, D. L., *Structural Electron Crystallography*. Plenum Press, New York, 1995.
13. Zou, X. D., Sukharev, Yu. and Hovmöller, S., *Ultramicroscopy*, 1993, **49**, 147–158.
14. Drenth, J., *Principles of Protein X-ray Crystallography*. Springer-Verlag, New York, 1994, p. 290.
15. Hauptman, H. A., *Crystal Structure Determination. The Role of the Cosine Seminvariants*. Plenum Press, New York, 1972, p. 386.
16. Germain, G., Main, P. and Woolfson, M. M., *Acta Cryst.*, 1970, **B26**, 274–285.
17. Rogers, D., *Theory and Practice of Direct Methods in Crystallography*, ed. M. F. C. Ladd and R. A. Palmer. Plenum Press, New York, 1980, pp. 23–92.
18. Sayre, D., *Acta Cryst.*, 1952, **5**, 60–65.
19. Stanley, E., *Acta Cryst.*, 1986, **A42**, 297–299.
20. Hu, H. L. and Dorset, D. L., *Acta Cryst.*, 1989, **B45**, 283–290.
21. Karle, I. L., Dragonette, K. S. and Brenner, S. A., *Acta Cryst.*, 1965, **19**, 713–716.
22. Kitaigorodskii, A. I., *Organic Chemical Crystallography*. Consultants Bureau, New York, 1961.
23. Amoros, J. L. and Amoros, M., *Molecular Crystals. Their Transforms and Diffuse Scattering*. John Wiley and Sons, New York, 1968.
24. Buerger, M. J., *Crystal Structure Analysis*. John Wiley and Sons, New York, 1960, p. 192.
25. Koch, E., *International Tables for Crystallography*, ed. A. J. C. Wilson. Kluwer, Dordrecht, 1995, pp. 10–14.

26. Geil, P. H., *Polymer Single Crystals*. John Wiley and Sons, New York, 1963, p. 60.
27. Hamilton, W. C., *Statistics in Physical Science*. Ronald Press, New York, 1964, pp. 157–162.
28. Dorset, D. L., Hu, H. L. and Jäger, J., *Acta Cryst.*, 1991, **A47**, 543–549.
29. Lotz, B., *Amer. Chem. Soc., Div. Polymer Chem., Inc. Preprints*, 1996, **37**(2), 430–431.
30. Puterman, M., Kolpak, F. J., Blackwell, J. and Lando, J. B., *J. Polym. Sci. Polym. Phys. Ed.*, 1997, **15**, 805–819.
31. Fisher, R. G. and Sweet, R. M., *Acta Cryst.*, 1980, **A36**, 755–760.
32. Carr, P. D., Cheah, E., Suffolk, P. M., Vasudevan, S. G., Dixon, N. E. and Ollis, D. L., *Acta Cryst.*, 1996, **D52**, 93–104.
33. Bragg, W. L. and Claringbull, C. F., *Crystal Structures of Minerals*. Bell, London, 1965, p. 86.
34. Ramachandran, G. N. and Srinivasan, R., *Fourier Methods in Crystallography*. John Wiley and Sons, New York, 1970, pp. 62–67.